Cs immobilization by sintered lead iron phosphate glasses

S.T. Reis, J.R. Martinelli *

Brazilian Nuclear Energy Commission, Energy and Nuclear Research Institute, C.P. 11049 Pinheiros, CEP 05422-970 São Paulo, SP, Brazil

Abstract

Lead iron phosphate glass frits were obtained from a mixture of $NH_4H_2PO_4$, PbO and Fe_2O_3 melted in an induction furnace. After milling, the material was pressed in a die, sintered, and sintered a second time. Three amorphous X-ray diffraction halos were observed in samples produced from non-homogenized powders while two halos were observed from homogeneous ones. These halos were assigned different phosphate compounds. Sintered pellets were immersed in a CsCl aqueous solution and the absorption of Cs was determined by scanning electron microscopy. The crystallization temperatures and activation energies were determined by differential thermal analysis and by the Kissinger Method, respectively. The weight loss and atomic absorption were used to measure the dissolution rate in deionized water. The weight loss of sintered glasses was 3×10^{-2} g/m^2 d after 28 days at 90°C. The homogenized samples have an improved corrosion resistance. © 1999 Elsevier Science B.V. All rights reserved.

1. Introduction

Glass powders can be used to immobilize nuclear wastes [1] if they are mixed, pressed, and heat treated to reduce the porosity and to aggregate the waste particles. This process is called vitrification of nuclear wastes, even though this term is commonly used when both glass and waste particles are melted together and cooled to form blocks [2]. Glass particle sintering is useful because glasses are chemically stable [3], are corrosion resistant [4], and do not degrade easily under radiation [2]. The sintering process also avoids exposing nuclear wastes to high temperatures required by a melting process. Hence the loss of contaminants by volatilization and chemical attack of the containers are reduced. The most common glass materials used in the vitrification processes are borosilicates with several different compositions, being hot or cold pressed and finally sintered [1]. Porous materials have also been investigated to immobilize nuclear wastes in the liquid state. Diatomite and shamote are examples [5].

Lead iron phosphate (LIP) glasses were first developed for radioactive storage in 1984, by mixing with nuclear waste compounds and then melting. These materials had a dissolution rate in water of 10^{-2} g/m^2 d revealing an important feature for materials that were intended for that application. The rate of dissolution decreased as the solution pH increased. In salted water solution, the LIP glasses dissolution rate was larger [6].

It was also noticed that these glasses could be used in other applications by modifying their composition. Glasses with thermal expansion coefficients of 18×10^{-6}/°C and relatively large refractive index (1.75–1.83 for visible spectrum) could be obtained. These materials can be potentially used in the sealing of ceramic to metals [7],

---

* Corresponding author. Tel.: +55-11 816 9346; fax: +55-11 816 9370; e-mail: jroberto@net.ipen.br

and laser hosts and optical fibers [8]. Recently it has been suggested that these glasses can also be used as nuclear particle detectors [9].

Chemical and physical properties of LIP glasses depend on the glass composition. The P_2O_5 is assumed to be the glass former and PbO is added to reduce the viscosity and consequently the melting point. By adding Fe_2O_3 it was possible to improve the chemical resistance and to decrease the crystallization rate [10]. The structure of LIP glasses consists of Fe–O–P–O chains with Pb atoms intercalating the structure, bounded to non-bridging oxygen atoms. Iron can exist in two valence states as Fe^{2+} and Fe^{3+} [3], so properties of LIP glasses depend on the melting condition.

The aim of the present paper is to investigate the chemical resistance of sintered LIP glasses after CsCl absorption from an aqueous solution by measuring the weight loss, and to compare their chemical resistance to that of glasses produced in different processing conditions. Differential thermal analysis (DTA) was used to determine the major temperatures related to the crystallization process. By varying the heating rate, ϕ, the variation of the temperature of crystallization, T_p, and the activation energy, E_c, could be measured. The results of DTA are discussed on the basis of the modified Kissinger's expression for superficial crystallization [11].

2. Experimental procedure

The LIP glass powders were produced by melting and quenching appropriate chemical compounds to obtain glass frits. This material was then milled and sieved to reach a suitable particle size distribution. The material so produced was intended to be used in the vitrification of liquid wastes. Powders were pressed and sintered leading to porous pellets that were immersed in a liquid solution containing cesium chloride, and finally sintered again.

2.1. Glass powders

The LIP glass powders were obtained as frits by mixing and melting 60.3 mol% $NH_4H_2PO_4$, 30.9

mol% PbO and 8.8 mol% Fe_3O_3 and finally quenching to room temperature. Melting was performed in argon with and without homogenization in an alumina crucible placed in the center of an induction furnace coil (Fig. 1). To heat the material, a graphite crucible was placed externally to the alumina one. Argon was used as the working atmosphere, so the graphite could be preserved. Initially the material was heated to 450°C and soaked for 1 h to convert $NH_4H_2PO_4$ to P_2O_5, reducing the amount of NH_3 during the melting. Therefore, the working atmosphere was slightly reducing. After that, the material was heated to 1050°C at 17.5°C/min and soaked for 1 h at that temperature. Frits were obtained by pouring the viscous liquid in a water tank. The selected composition was the same used in other work [12].

2.2. Powders processing

Powders were ground by ball milling for 30 h using alumina as grinding medium. The material was then uniaxially pressed in a 10 mm diameter die at 100 MPa. The internal walls of the die were previously lubricated with zinc stearate to reduce the friction between the powder and the walls. Therefore a more uniform internal stress distri-
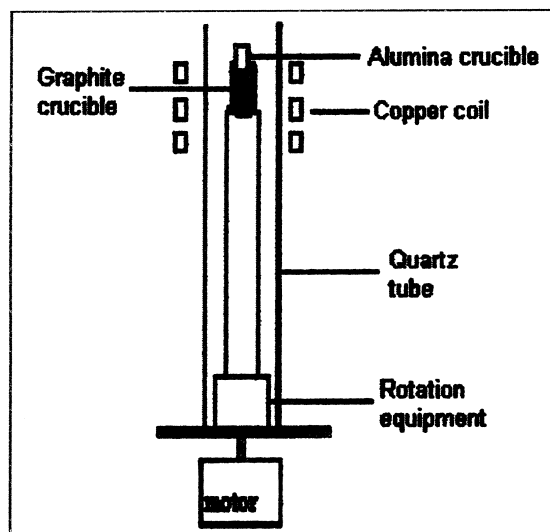

Fig. 1. System for material homogenization.

bution could be reached and the resulting pellets could be easily pulled from the die. After pressing, samples were heated to 400°C and soaked for 1 h, cooled to room temperature, immersed in a CsCl solution (4.8M) for 2 s, and dried in air for 24 h. The final densification was performed at 780°C (samples homogenized with Cs), 800°C (samples homogenized without Cs), and 750°C (samples non-homogenized with and without Cs) in air by using an electrical furnace. Samples were heated at 20°C/min to those temperatures, and cooled down to room temperature at 22°C/min. No soaking was performed at those temperatures.

X-ray diffraction (XRD) and scanning electron microscopy (SEM) were performed to identify crystalline and amorphous phases in the material. A diffractometer (Philips model PW 3710) and a scanning electron microscope (Philips model XL 30) were used for that purpose. To determine the temperature related to the maximum crystallization, T_p, and the melting temperature of the crystalline phase, T_m, thermal analyses were performed in nitrogen by using thermal analysis instruments

(T A model 2100 and Netzsch model STA 4099 C/7/E) adopting three different heating rates: 10, 15 and 20°C/min.

3. Results

3.1. Powder properties

Fig. 2 shows the XRD patterns from the LIP glass powders before milling.

Table 1 shows the LIP glass powder composition for non-homogenized (S1) and homogenized (S2) samples determined by the X-ray fluorescence analyses.

Table 2 shows densities for glass powders determined by helium picnometry.

The medium particle size is 3.23 μm.

3.2. LIP glasses with and without Cs

3.2.1. DTA analysis

Figs. 3 and 4 show differential thermal analyses patterns obtained for LIP glass pellets (sintered once) that have or not been immersed in a cesium chloride solution, respectively.

3.2.2. Chemical durability

Table 3 shows the weight loss (ΔR_i), and pH's of solutions where glass pellets (sintered twice) were kept during the leaching tests performed according to the Materials Center of Characterization (MCC-P1) [13].

Figs. 5 and 6 show scanning electron micrographs of sintered glass samples with Cs after leaching tests and thermal etching at 700°C in air for 20 min.

Fig. 7 shows the energy-dispersive X-ray spectroscopy (EDS) Cs dot map for an LIP glass sample previously immersed in a CsCl aqueous solution (4.8M) for 15 s.
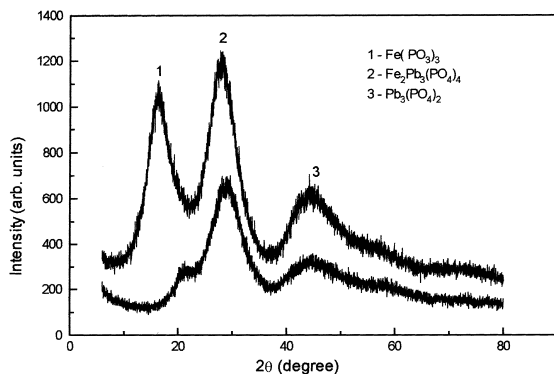
Fig. 2. X-ray diffraction patterns for non-homogenized (S1) and homogenized (S2) LIP glass powders.

Table 1
Composition of LIP in mol% determined by X-ray fluorescence analyses

Sample code	Precursors (mol%)			After melting (mol%)		
	$NH_4H_2PO_4$	PbO	Fe_2O_3	P_2O_5	PbO	Fe_2O_3
S1/S2	60.3	30.9	8.8	43.6	43.6	12.8

Table 2
Densities determined by helium picnometry

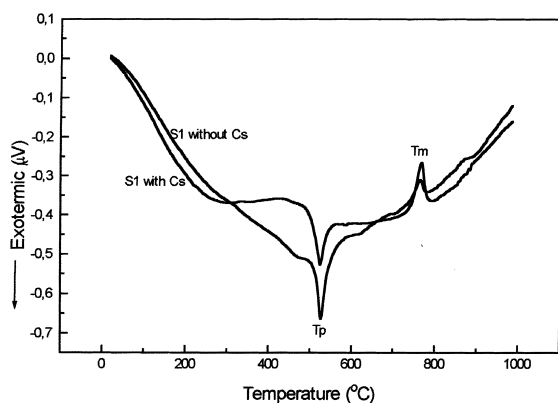| Sample code	Melting temperature (°C)	Soaking time (h)	Density (g/cm^3)
S1	1050	1	5.30 ± 0.02
S2	1050	3	5.22 ± 0.03

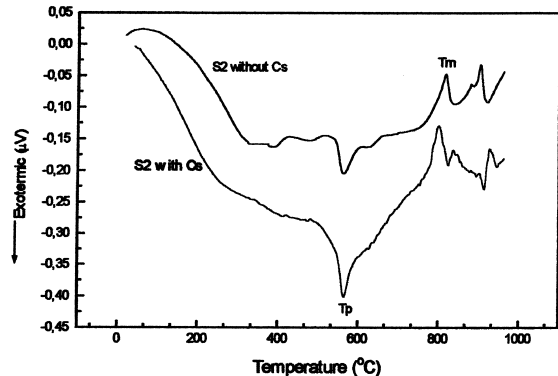Fig. 3. Differential thermal curves for non-homogenized LIP glasses with and without Cs (heating rate: 10°C/min).

Fig. 4. Differential thermal curves for homogenized LIP glasses with and without Cs (heating rate: 10°C/min).

Table 3
Weight loss $(\Delta R_i)_c$ pH after leaching

Sample code	pH (after 28 days)	ΔR_i (g/m^2 d) × 10^2
S1 with Cs	7.1	(5.0 ± 0.1)
S2 with Cs	6.8	(3.0 ± 0.2)
V01 [a]	6.8	1
V02 [b]	–	4

[a] V01 LIP glasses with nuclear waste simulators [4].
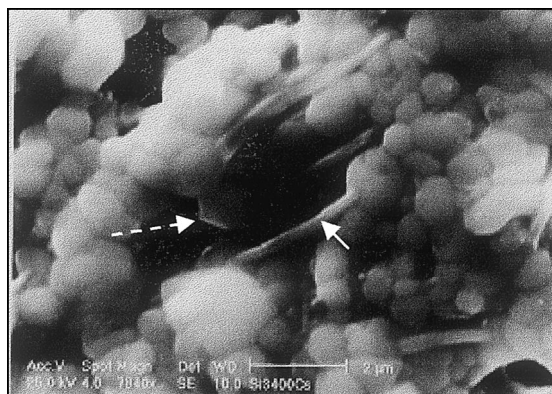[b] V02 borosilicate glasses with nuclear waste simulators [1].

Fig. 5. Scanning electron micrograph from the S1 type glass with Cs after leaching at 90°C during 28 days in distilled water.
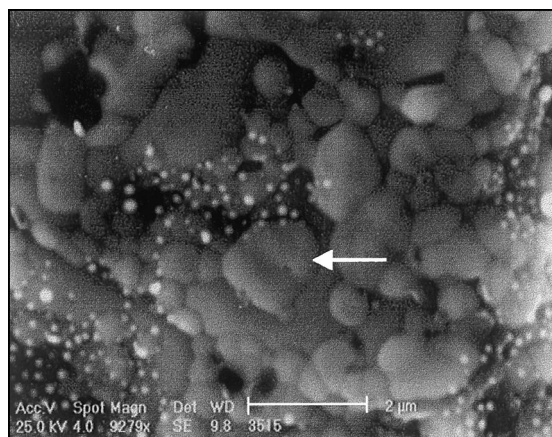

Fig. 6. Scanning electron micrograph from the S2 type glass with Cs after leaching at 90°C during 28 days in distilled water.

4. Discussion

4.1. Powder processing

No crystalline phases were observed in XRD patterns shown in Fig. 2. Three amorphous XRD halos can be seen in non-homogenized samples (S1) which correspond to ferric metaphosphate, $(Fe(PO_3)_3$ (halo #1), lead iron phosphate, $Fe_2Pb_3(PO_4)_4$ (halo #2), and lead orthophosphate, $Pb_3(PO_4)_2$ (halo #3). In homogenized samples (S2), only halos #2 and #3 were observed.
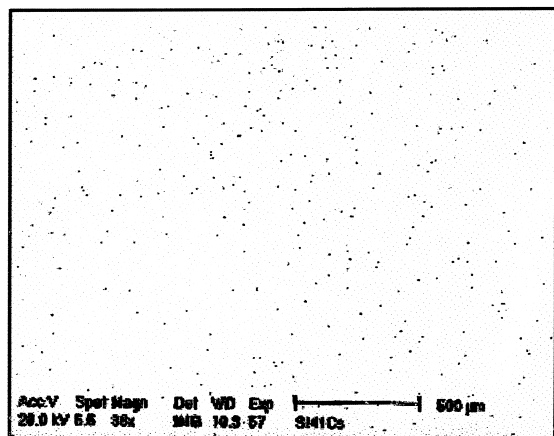
Fig. 7. Energy-dispersive X-ray spectroscopy (Cs dot map).

From Table 1 we note that approximately 81 mol% of $NH_4H_2PO_4$ was converted to P_2O_5. Ammonia and water were also evolved during the process.

4.2. DTA analysis

From the DTA we infer that Cs does not change the crystallization peak temperature for either sample (see Table 4). However, for the S2-type glass, the melting temperature of the crystalline phases formed during the DTA is split (Fig. 4). The material was sintered in a temperature relatively low to allow the incorporation of Cs as a modifier in the glass network (S2 glass type). The T_ms change is related to impurities introduced in the crystal lattice during the immersion in cesium chlorine solution. The XRD patterns (not presented here) showed the presence of

$Pb_5(PO_4)Cl$. T_ms determined by DTA indicate the maximum sintering temperatures allowed if material softening is to be avoided.

The original Kissinger equation is only valid for predominantly surface crystallization or when crystal growth occurs on a fixed number of nuclei. This means that, when a glass crystallizes predominantly by surface crystallization (for example, glasses consisting of very fine particles), fitting the maximum crystallization temperature as a function of heating rate with the original Kissinger equation will yield the activation energy suitable for the adopted model [11]. It has been shown that lead iron phosphate glass powders (type S1 and S2) with particle sizes smaller than 35 μm show predominantly surface crystallization [15]. Since the particle sizes of glasses type S1 and S2 are smaller than 35 μm (see Table 5), the original Kissinger equation [11] should be adopted:

$$\ln(\phi/T_p^2) = -E_c/RT_p + k. \tag{1}$$

In this equation T_p is related to E_c (parameter related to the activation energy for crystallization) and to a constant, k; ϕ is the DTA heating rate, 10, 15 and 20°C/min in the present investigation.

Table 5
Densities from sintered S1-type glasses as a function of heating rate. The initial medium particle size was kept constant to 3.67 μm

Heating Rate (°C/min)	Density (%DT)
5.0	89 ± 0.4
10.0	90 ± 0.5
15.0	94 ± 0.6
20.0	98 ± 0.4

Table 4
Densities, crystallization activation energy and relevant temperatures for samples with and without Cs

Sample code	T_p (°C)	T_m (°C)	E_c (kJ/mol)	Density (% TD)
S1	526	767	116 ± 15	98 ± 0.5
S1 with Cs	526	767	93	90 ± 0.3
S2	565	820	131	98 ± 0.6
S2 with Cs	565	800	116	94 ± 0.5
$Se_{76}Sb_6Te_{20}$ [a]	416	–		

[a] Material for comparison purpose [14].

Figs. 8 and 9 show a plot of $\ln(\phi/T_p^2)$ as a function of $1/T_p$ for T_ps obtained from the DTA performed at different heating rates. From the curve slopes, E_{ck}s are calculated.

Table 4 shows T_p and T_m for $\phi = 10°C/min$ and densities determined by the Archimedes method. The activation energy for crystalline phase formation E_c was calculated from the curve slope [11]. These E_cs are shown in Table 4 too. We also note that the addition of Cs leads to smaller E_cs, and consequently smaller final densities.
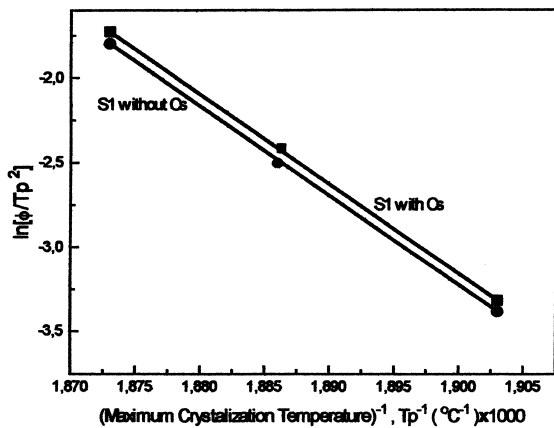

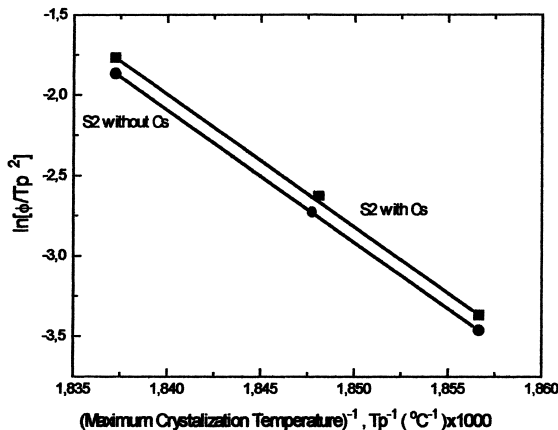Fig. 8. Plot of $\ln(\phi/T_p^2)$ as a function of $1/T_p$ for S1-type glass with and without Cs.

Fig. 9. Plot of $\ln(\phi/T_p^2)$ as a function of $1/T_p$ for S2-type glass with and without Cs. Lines are drawn as guides for the eyes.

4.3. Chemical durability

In the S1 type samples we note the presence of $Fe_2Pb_3(PO_4)_4$ agglomerates, $Pb_3(PO_4)_2$ with needle shapes (indicated by an arrow in Fig. 5), and $(Pb_5(PO_4)_3Cl)$ crystals with hexagonal shapes (indicated by a broken arrow in Fig. 5). In the S2 type samples we also note the presence of large $Fe_2Pb_3(PO_4)_4$ agglomerates (indicated by an arrow in Fig. 6), and whitish grains that were identified as P-rich phases by EDS analyses. No $(Pb_5(PO_4)_3Cl)$ crystals or $Pb_3(PO_4)_2$ needles have been found in these materials. All crystalline phases observed in the present work were previously identified [10].

Data from Table 3 show that the S2 type samples are a promising material for use in the immobilization of Cs since they have a minor weight loss during the leaching tests comparable to LIP glasses previously obtained by melting [4]. Furthermore, the leaching tests show that this material can be considered better than the S1 glass type and even sintered borosilicate glasses [1]. The leaching solutions where S1 type samples were kept show a larger pH variation compared to the one where S2 type samples were exposed. This fact might be related to the hydration and releasing of phosphate chains in the solution where the S1 samples were kept, since a 'non-bridging' oxygen in the S1 type samples may hydrolyze the phosphate chains.

Fig. 7 shows a non-homogeneous distribution of Cs atoms that probably occupied specific positions on the surface boundaries of glass particles prior in the final sintering process. Apparently there was no Cs diffusion in the glass matrix.

5. Conclusions

Homogenized frits are shown to improve those properties affected by the leaching tests, increase densities, and inhibit crystallization. Activation energies determined by Kissinger method for all LIP glasses are comparable to the ones previously reported in the literature for phosphate glasses. S2 type glasses are promising materials for waste immobilization because they show better chemical durability when compared to S1 type glasses and

others. The leaching test results show that S2 type glasses containing Cs have a greatest chemical resistance to aqueous solution than do S1 type glasses.

Acknowledgements

References

[1] D.O. Russo, N.B.M. de Bernasconi, J. Nucl. Mater. 22 (1995) 151.
[2] I.W. Donald, B.L. Metcalfe, R.N.J. Taylor, J. Mater. Sci. 32 (1997) 5851.
[3] C.S. Ray, X. Fang, D.E. Day, in: Chemical Durability, Crystallization, and Iron Redox Equilibria of Iron Phosphate Glasses, J. Non-Cryst. Sol., 1998.
[4] B.C. Sales, L.A. Boatner, Matter. Letts. 2 (1984) 301.
[5] L.N. Lazarev et al., Ceramics nuclear waste management, in: T.D. Chikalla, J.E. Mendek (Eds.), Cincinatti, Conf-790420, Technical Information Center, 1979, p. 179.
[6] B.C. Bunker, J.A. Wilder, J. Non-Cryst. Solids 64 (1984) 291.
[7] Y. Peng, D.E. Day, Glass Technol. 32 (5) (1991) 166.
[8] W.S. Key, J.C. Miller, Advanced Photonics at ORNL: Shedding Light on a New Initiative, ORNL Rev. 27 (3) (1994) 3.
[9] S. Wang, A.J. Westphal, Nucl. Instrum. and Meth. B35 (1988) 43.
[10] B.C. Sales, M.M. Abraham, J. Non-Cryst. Solids 71 (1985) 103.
[11] K. Matusita, S. Sakka, J. Non-Cryst. Solids 38&39 (1980) 741.
[12] S.T. Reis, J.R. Martinelli, Proceedings of the XII Brazilian Materials Science and Engineering Congress, Aguas de Lindoia, SP 1 (1996) 101.
[13] Nuclear Waste Material Handbook. Waste Forms Test Methods, Report DOE/TIC 11400, Materials Characterization Center, USA, 1981.
[14] R.M. Mehra, G. Kaur, J. Mater. Sci. 26 (1991) 3343.
[15] S.T. Reis, PhD thesis, University of São Paulo, 1999.